euronoise

Panel transmission measurements: the influence of the non plane wave nature of the incident field

Victor Humphrey[a] and John Smith[b]

[a]Institute of Sound and Vibration, Univ. of Southampton, University Road, Highfield, SO17 1BJ Southampton, UK
[b]DSTL, Rm 14, Bldg 352, Porton Down, SP4 0JQ Salisbury, UK
vh@isvr.soton.ac.uk

For reasons of cost and practicality, the laboratory measurement of the acoustic transmission and reflection properties of materials for use in underwater applications are typically performed on samples of limited dimensions — and with the source and receiver separated by relatively short distances — resulting in a non-planar measurement field. The influence of this on the resulting measurements is investigated in this paper. In particular, for low frequency measurements the influence of the evanescent wave contributions can become significant.
In this paper two alternative approaches are used to evaluate the transmission properties. The first approach uses an asymptotic expansion of the fields in terms of wave front curvature: bounds are then placed on the error in this expansion at low frequency using thin plate theory. The second method decomposes the incident spherical wave into its plane wave components and integrates the resulting transmitted waves numerically to evaluate the transmitted field. Results are compared and contrasted for measurements in the frequency range 1 to 60 kHz for panels of simple elastic materials (steel and Perspex (Poly(methyl methacrylate))). In addition the nature and significance of the modes of the panel for evanescent waves are considered. The consequences for laboratory measurements are also outlined.

1 Introduction

The reflection and transmission coefficients of a plane wave incident on an infinite panel provide a convenient means of characterising the acoustic properties of a material. These are often measured using a limited size panel; the finite size of the panel and measuring system then impose limitations on the measurement. Of the different sources of error, this paper is concerned with those caused by the non-plane wave nature of the source. That spherical wave components can cause deviations of the measured transmission coefficient from the plane wave result has been demonstrated before: in [1, 2] it was shown that the plane wave spectrum of the source can cause errors at high frequency, but the frequencies considered were higher than those typically of interest in many applications. A numerical study by Piquette [3] indicated the presence of a potentially large, low frequency effect. This was further studied by Shenderov [4, 5]; these calculations show a much smaller effect than that seen in [3].

In this paper the effect of an incident spherical wave on a measurement of the transmission coefficient is re-examined. It is shown that the transmitted pressure can be written as an asymptotic expansion of the wavenumber multiplied by the separation between the source and the receiver, the first term of which gives the plane wave transmission coefficient. When the plate is thin, explicit analytic bounds are found on the error in this expansion; these bounds suggest that, in order to ensure that a measurement gives a reasonable approximation to the plane wave transmission coefficient of a thin plate, the separation between the source and receiver needs to be larger by a factor of the fluid loading parameter than that which would be deduced by looking at the asymptotic expansion alone. These bounds allow effects of the order of those seen in [3] for some materials: in order to examine the discrepancy between [3] and [4] the plane wave spectrum is integrated using the full elastic transmission coefficient. This gives results in agreement with [4].

2 Asymptotic analysis and error bounds

The starting point is to express the reflection and transmission coefficients in terms of integrals over the plane wave spectrum of the source. Consider a plate of thickness, h, lying at the origin in the $r-\phi$ plane of a cylindrical co-ordinate system, (r, ϕ, z). It is surrounded on both sides by an acoustic fluid of sound speed c, and is insonified using a monopole source of angular frequency ω, positioned at $(0, 0, z_0)$. The incident pressure field along the z-axis, for $z < z_0$, is thus given by

$$p_i(z) = \frac{a_0}{\mathrm{i}} \int_0^\infty \frac{1}{\beta} e^{\mathrm{i}\beta(z_0-z)} \alpha \, \mathrm{d}\alpha = -\frac{a_0}{R} e^{\mathrm{i}kR} \qquad (1)$$

where $k = \omega/c$, $R = z_0 - z$ and an overall time dependence on $\exp(-\mathrm{i}\omega t)$ has been ignored. The branch cut for $\beta = \sqrt{k^2 - \alpha^2}$ must be chosen such that $\beta = \mathrm{i}\sqrt{\alpha^2 - k^2}$ as $\alpha \to \infty$.

Using these definitions the reflected pressure, p_r, and the transmitted pressure, p_t, can be written as

$$p_r(z) = \frac{a_0}{\mathrm{i}} \int_0^\infty \frac{1}{\beta} R(\alpha) \, e^{\mathrm{i}\beta(z+z_0)} \alpha \, \mathrm{d}\alpha \qquad (2)$$

and

$$p_t(z) = \frac{a_0}{\mathrm{i}} \int_0^\infty \frac{1}{\beta} T(\alpha) \, e^{\mathrm{i}\beta(z_0-z)} \alpha \, \mathrm{d}\alpha. \qquad (3)$$

$R(\alpha)$ and $T(\alpha)$ are then found by satisfying the stress and displacement boundary conditions on the faces of the plate [3]. For propagating components ($\alpha < k$), they are the reflection and transmission coefficients.

Attention will now be restricted to the transmission coefficient, although similar results can be obtained for the reflection coefficient. First the integral in (3) is split into two parts — an integral over $\alpha < k$ and an integral for $\alpha > k$:

$$\begin{aligned} p_t(z) = & \frac{a_0}{\mathrm{i}} \int_0^k \frac{1}{\beta} T(\alpha) e^{\mathrm{i}\beta R} \alpha \, \mathrm{d}\alpha \\ & + \frac{a_0}{\mathrm{i}} \int_k^\infty \frac{1}{\beta} T(\alpha) e^{\mathrm{i}\beta R} \alpha \, \mathrm{d}\alpha. \end{aligned} \qquad (4)$$

In the first integral the change of variable $u = \beta/k$ is made. The result is a Fourier integral whose asymptotics can be treated using integration by parts [6]. For the

second integral (the integral over the evanescent part of the spectrum), changing variables to $u = \beta/\mathrm{i}k$ gives an integral that can be treated using Watson's Lemma [6]. Defining $\hat{T}(u) = T(k(1-u^2)^{\frac{1}{2}}) \equiv T(k\cos\theta)$ (where θ is the angle from the normal to the panel), these integrals become

$$\begin{aligned} I_1 &= \frac{a_0 k}{\mathrm{i}} \int_0^1 \hat{T}(u)\, e^{\mathrm{i}kR\,u}\mathrm{d}u \\ &= -\frac{a_0 e^{\mathrm{i}kR}}{R}\left(\hat{T}(1) - \frac{1}{\mathrm{i}kR}\hat{T}'(1)\right) \\ &\qquad - \frac{a_0\hat{T}'(0)}{\mathrm{i}kR^2} + \frac{a_0 k}{\mathrm{i}}\epsilon_1 \end{aligned} \tag{5}$$

and

$$\begin{aligned} I_2 &= -a_0 k \int_0^\infty \hat{T}(\mathrm{i}u)\, e^{-kR\,u}\mathrm{d}u \\ &= \frac{a_0\hat{T}'(0)}{\mathrm{i}kR^2} + \frac{a_0 k}{\mathrm{i}}\epsilon_2, \end{aligned} \tag{6}$$

were use has been made of the fact that $\hat{T}(0) = 0$.

Putting these two results together, the contribution from the limit at $u = 0$ from the propagating integral, I_1, cancels the contribution from the limit in the evanescent integral, I_2. This can be shown to be true at all orders of the asymptotic expansion. The result is (ignoring contributions of $O(h/R)$)

$$p_t = -\frac{a_0}{R}e^{\mathrm{i}kR}\left\{\hat{T}(1) - \frac{1}{\mathrm{i}kR}\hat{T}'(1)\right\} + \frac{a_0 k}{2\mathrm{i}}\left(\epsilon_1 + \epsilon_2\right). \tag{7}$$

This result is exact and the error terms ϵ_1 and ϵ_2 are given by

$$\epsilon_1 = -\frac{1}{(kR)^2}\int_0^1 \hat{T}''(u)\, e^{\mathrm{i}kR\,u}\mathrm{d}u, \tag{8}$$

and

$$\epsilon_2 = \frac{1}{\mathrm{i}}\int_0^\infty \left(\hat{T}(\mathrm{i}u) - \mathrm{i}\hat{T}'(0)u\right) e^{-kR\,u}\mathrm{d}u. \tag{9}$$

The term in curly brackets in Eq. 7 is the measured transmission coefficient, T_m. Due to the theorems governing the asymptotic forms of ϵ_1 and ϵ_2 implicit in Watson's Lemma and integration by parts [6], it can be seen that

$$T_m \sim \hat{T}(1) - \frac{1}{\mathrm{i}kR}\hat{T}'(1) + o\left(\frac{1}{kR}\right), \quad \text{as } kR \to \infty. \tag{10}$$

Thus the leading order spherical correction to the measured transmission coefficient depends on the rate of change of the plane wave transmission with angle, as has been observed previously [1, 4]. It is tempting to try to use (10) to determine the separation needed to ensure that the corrections are smaller than a given accuracy [4], however this is incorrect: the result (10) is a statement about the limit $kR \to \infty$. To estimate how accurately (10) holds bounds must be found on the error terms, ϵ_1 and ϵ_2. Since these bounds necessitate an analysis of the pole structure of $\hat{T}(u)$ in the complex u plane, the plate is now assumed to be thin. In this case the poles are found to be related to the dispersion curves of a fluid loaded thin plate. Crighton has shown how approximate expressions for the bending wave solutions could be found by expanding in the fluid loading parameter ε, which is given by

$$\varepsilon = \frac{\rho_0}{mc}\sqrt{\frac{B}{m}}, \tag{11}$$

where ρ_0 is the density of the fluid, m is the mass per unit area of the plate and B is its bending stiffness. Physically this is the ratio of the mass loading of the fluid to the mass of the plate at the coincidence frequency and is always expected to be a small parameter for rigid plates [7]. This analysis was recently extended to include the symmetric wave solutions [8].

It is useful to introduce $\bar{\omega}$, which is the frequency scaled to the coincidence frequency on the plate, the parameters α_l and α_p (defined in [8]) and $\delta = c^2/c_p^2$. The transmission coefficient is then given by

$$\begin{aligned} \hat{T}(u) = &\frac{2\mathrm{i}\varepsilon u}{\bar{\omega}C(u)D(u)}\big[(1-u^2-\delta) \\ &+ \alpha_p\bar{\omega}^2(1-u^2)\left(1-\bar{\omega}^2(1-u^2)^2\right) \\ &+ \alpha_l\bar{\omega}^2(1-u^2-\delta)\left(1-\bar{\omega}^2(1-u^2)^2\right)\big] \end{aligned} \tag{12}$$

where

$$C(u) = \left[u(1-\bar{\omega}^2(1-u^2)^2) + \frac{2\mathrm{i}\varepsilon}{\bar{\omega}}\right] \tag{13}$$

and

$$\begin{aligned} D(u) = \big[&(1-u^2-\delta)(u - 2\mathrm{i}\varepsilon\alpha_l\bar{\omega}) \\ &- 2\mathrm{i}\varepsilon\alpha_p\bar{\omega}(1-u^2)\big]. \end{aligned} \tag{14}$$

Maxima in the transmission coefficient and its derivatives are associated with the factors $C(u)$ and $D(u)$ in the denominator getting small. Since ε is expected to be small ($\varepsilon \simeq 0.13$ for steel in water and $\varepsilon \simeq 0.3$ for Poly(methyl methacrylate) (PMMA) in water), the peaks in $\hat{T}''(u)$ are near $u = 0$ and $u^2 = 1-\delta$ providing $\bar{\omega} < 1$ (and $\bar{\omega} = O(1)$). An estimate of ϵ_1 is thus obtained by separating out these peaks and then placing a crude bound on the remaining integral. The contribution from the peaks is then included as the maximum value of the peaks multiplied by their width. Thus,

$$\begin{aligned} |\epsilon_1| \lesssim \frac{1}{(kR)^2}\Bigg\{ &\frac{\sigma}{2\varepsilon^2\bar{\omega}^2\left(\alpha_l + \frac{\alpha_p}{1-\delta}\right)^2} + \frac{4(1-\delta)\sigma}{\varepsilon^2\alpha_p^2\delta^2\bar{\omega}}\left[1 + O(\varepsilon^2)\right] \\ &+ \frac{\bar{\omega}(1-3\sigma)}{2\varepsilon^2}\left[\bar{\omega}^2\left(1+4\bar{\omega}^2\right)^2 + 64\varepsilon^2\right]^{\frac{1}{2}}\Bigg\} \end{aligned} \tag{15}$$

for some $\sigma > \varepsilon^2\bar{\omega}^2[(1-\delta)\alpha_l + \alpha_p]^2$.

Things are slightly more complicated for ϵ_2; there are two poles on the path of integration (in the case of no material damping), as can be seen from the plot of T over the evanescent part of the plane wave spectrum shown in Fig. 1. One is at

$$u \sim \sqrt{\frac{1}{\bar{\omega}} - 1}\left(1 + \frac{\varepsilon}{2(1-\bar{\omega})^{\frac{3}{2}}} + O(\varepsilon^2)\right), \tag{16}$$

($\bar{\omega} = O(1)$) which is associated with coupling into the subsonic mode in the plate for $\bar{\omega} < 1$. The other looks

like a Scholte-Stoneley wave and is at

$$u \sim 2\varepsilon\alpha_l\bar{\omega} + \frac{2\varepsilon\alpha_p\bar{\omega}}{1-\delta}\left(1 - \frac{4\delta\bar{\omega}^2\varepsilon^2}{1-\delta}\left[\alpha_l + \frac{\alpha_p}{1-\delta}\right]^2 + O(\varepsilon^4)\right). \quad (17)$$

It is a coupled fluid-plate mode formed by coupling into the plate at near grazing incidence. The result may be evaluated using contour integration by deforming the path of integration onto a new path at 45° to the real u axis. The error ϵ_2 is then given by finding the maximum value of this (finite) path and adding the residues of the poles crossed in deforming the path. Using standard techniques [6] the result is found to be

$$|\epsilon_2| \lesssim \frac{\sqrt{2}}{(1-\delta)\varepsilon^2\bar{\omega}^2\left(\alpha_l + \frac{\alpha_p}{1-\delta}\right)^2 (kR - \sigma_n)^3 + \pi e^{-2kR\varepsilon\bar{\omega}(\alpha_l + \alpha_p/(1-\delta))}} \quad (18)$$

where

$$\sigma_n \simeq \frac{\ln 2}{4\varepsilon\bar{\omega}\left(\alpha_l + \frac{\alpha_p}{1-\delta}\right)} \quad (19)$$

and kR has been chosen so that $kR > \sigma_n$ (otherwise the estimate for ϵ_2 would depend on $1/(kR)^2$).

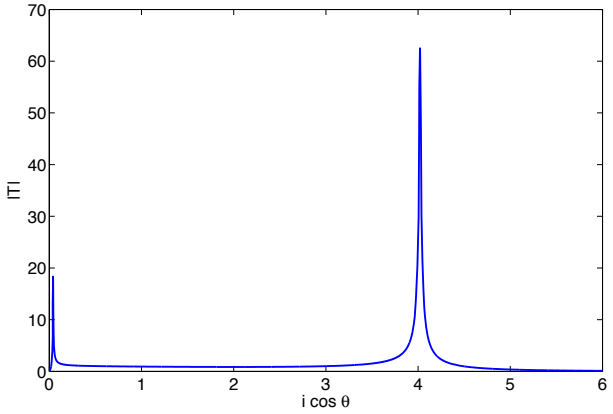

Figure 1: Plot of the modulus of the transmission coefficient for evanescent wave contributions showing the presence of peaks due to Scholte-Stoneley and subsonic modes.

Surprisingly, rather than being small when $kR > 1$ as one might expect from the asymptotic result (10), the error terms (15) and (18) have a functional dependence on εkR. This seems to imply that, in order to be certain spherical wave corrections can be ignored one needs to require $\varepsilon kR > 1$, rather than $kR > 1$ as would be deduced from the asymptotic result (10).

Fig. 2 shows a comparison of the thin plate transmission coefficient with the modulus of T_m from (10), together with the magnitudes of the bounds on ϵ_1 and ϵ_2 calculated using the parameters for PMMA in Section 3. This shows the close agreement of the asymptotic result to the plane wave result. The approximations used in deriving the bounds (15) and (18) break down for $\bar{\omega} = O(\varepsilon)$ hence the low frequency behaviour is not physical. Away from this region the bounds, though small, are larger than would be expected from (10) alone. When PMMA is replaced by steel however, the bounds on ϵ_1 and ϵ_2 become large (Fig. 3): these bounds would allow the effects seen in [3] however they are upper bounds on the error only and are expected to be conservative. To investigate the errors further requires a numerical approach.

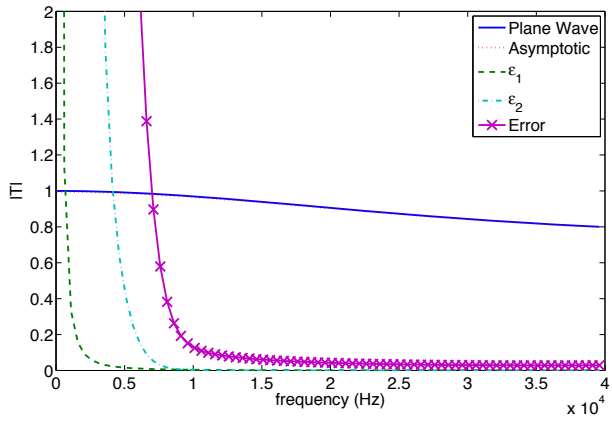

Figure 2: Comparison of the plane wave transmission coefficient with the first order spherical correction (10) for a Perspex panel. Also shown are the magnitudes of the error integrals, ϵ_1 and ϵ_2, and the associated error in T_m.

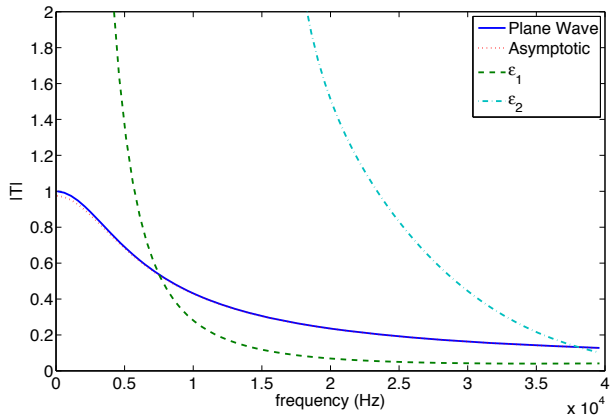

Figure 3: Plot of moduli of the plane wave transmission coefficient and first order spherical wave correction, together with magnitudes of the error integrals for a steel panel.

3 Numerical calculations

An alternative approach is to use numerical integration to obtain values for the transmitted pressure p_t from Eq.. (4). This enables the effective transmission coefficient to be calculated, which can be expressed as an Insertion Loss, IL, using $\mathrm{IL} = -20\log_{10}(|T_m|)$. The numerical integration of (4) is taken in two parts for convenience with the ranges being divided as necessary for efficiency. The transmission coefficient was implemented using the expressions in [9] with a correction for the water path replaced by the test panel.

Fig. 4 shows example calculations for a Perspex (PMMA) panel 0.0127 m in thickness measured at a

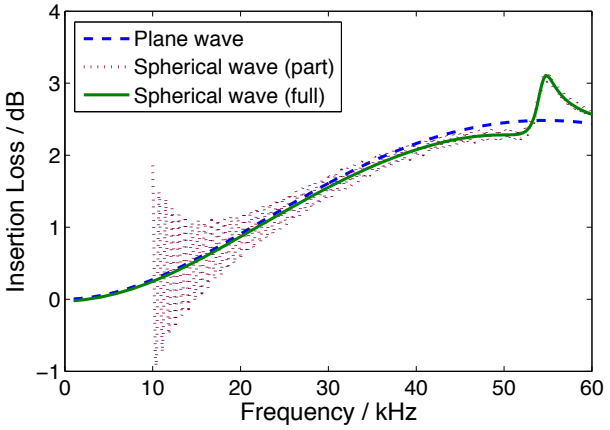

Figure 4: Calculated Insertion Loss for a 12.7 mm Perspex plate for a plane wave (dashed line) and spherical wave for a source-receiver distance of 2.0 m (solid line). The contribution from the real part of the spectrum for the spherical wave case is shown as a dotted line.

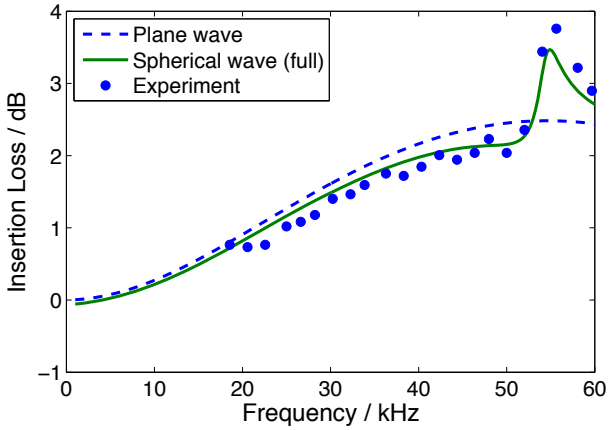

Figure 5: Comparison of calculated Insertion Loss for a 12.7 mm Perspex plate for a spherical wave and observation ranges of 2.0 m (solid line) and 0.9 m (dot-dashed line) with the plane wave result (dashed line).

distance of 2.0 m from the source. Note that the range of the test panel from the source is not significant. In this case the Insertion Loss for a plane wave increases steadily from 1 kHz with a smooth maximum at about 54.5 kHz. The result of the first integral in (4) is shown as a dotted line for frequencies above 10 kHz. This shows a distinct departure from the plane wave result between 50 and 60 kHz; with a maximum departure of about 0.6 dB. The results are, however, obscured by a significant oscillatory component that grows in amplitude as the frequency is reduced. This is the reason for only presenting the results above 10 kHz. This oscillation is associated with the non-zero contribution from the upper end of the integral over the real angle alpha. This disappears when both parts of the integration in (4) are performed, as the contribution from the lower limit of the imaginary integral almost completely cancels out that from the end of the real integral. The resulting Insertion Loss follows the plane wave result very closely for frequencies up to 20 kHz, and then lies slightly below the plane wave result until the significant deviation around 55 kHz.

This result indicates that at low frequencies the differences between the effective transmission coefficient for spherical waves and the plane wave transmission coefficient is very small. In this case less than 0.1 dB up to 20 kHz.

The existence of the specific deviation at 55 kHz has already been noted in [1]. In that case the transmission coefficient was predicted using an approximate solution for the effective transmission coefficient that was appropriate to a parametric array used as the source in [10]. In that case the integral was only performed over real angles and was, therefore, limited to frequencies above about 20 kHz. The experimental data obtained for a source-hydrophone separation of 0.9 m in [1] is compared with the results of the current calculation for a spherical wave incidence and a separation of 0.9 m in Fig. 5 .

Although not strictly equivalent (the experimental data were obtained for a parametric beam rather than a point source) the plots show a number of features in common. Firstly, over the range from 20 to 50 kHz both the experiment and the model indicate an Insertion Loss that is less than that for a plane wave. Secondly, both experiment and theory show a characteristic deviation from the plane wave result at about 55 kHz. The spherical wave approach underestimates the peak loss; however, if the apparent acoustic centre of the array is assumed to be at its mid point, shortening the apparent range, then the predicted loss increases.

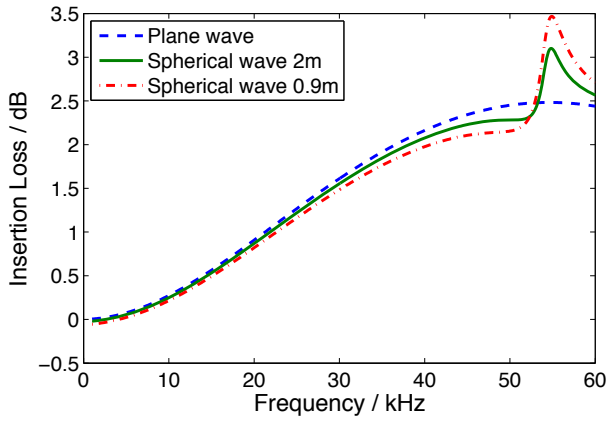

Figure 6: Comparison of calculated Insertion Loss for a 12.7 mm Perspex plate for a plane wave (dashed line) and for a spherical wave (solid line) with experimental results (points) obtained using a parametric array as a source [1]. The source-receiver distance is 0.9 m.

The spherical wave approach also predicts that the effective loss should smoothly decrease with reducing frequency, and be very similar to the plane wave result for the lowest frequencies. The effect of the measurement range is shown in Fig. 6 which presents numerical results for the effective spherical wave Insertion Loss for separations of 0.9 m and 2.0 m. This indicates how the peak loss at 55 kHz increases as the range reduces. It also shows that the underestimate of loss between 20 and 50 kHz increases as the separation reduces. Finally the results show that at the lowest frequencies there is

a small negative loss, i.e., a transmission coefficient of slightly greater than one for spherical wave. This effect is larger at shorter ranges and is attributed to the apparent change in position of the source caused by the panel.

The numerical evaluation of the integrals in (4) is more difficult for steel because of the lower material loss and hence reduced width of the Insertion Loss peaks contributing to the imaginary part of the integral. However the results presented in Fig. 7 show that the resulting Insertion Loss for the spherical wave case is very close to that for a plane wave, in agreement with [4].

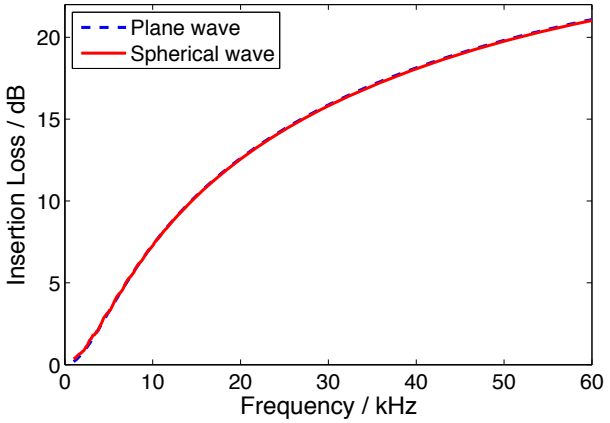

Figure 7: Comparison of calculated Insertion Loss for a 12.7 mm steel plate for a plane wave (dashed line) with that for a spherical wave (solid line) for a source-receiver distance of 2.0 m.

4 Discussion and Conclusions

The asymptotic expansion for the spherical wave transmission coefficient (10) depends only on the plane wave transmission coefficient and its derivatives at normal incidence and would give a pressure at the receiver that was lower, and thus a higher Insertion Loss, than would be obtained using a plane wave. The bounds on the error integrals however depend on the whole plane wave spectrum and turn out to be dominated by coupling into the longitudinal wave for the integral over the real part of the spectrum (ϵ_1) and the Scholte-Stoneley mode for the integral over the imaginary part of the spectrum (ϵ_2). The second of these would not be predicted by the usual thin plate analysis [7] — though it is seen in the numerical evaluation of the full elastic equations [5] — and arises in [8] through the matching of the acoustic pressure to the normal stress at the surface of the plate, allowing the formation of a Scholte-Stoneley type wave below the coincidence frequency in addition to the subsonic wave. Coupling into these modes can increase the pressure at the receiver above that for a normally incident plane wave.

These bounds are upper bounds on the error only, however numerical integration of the plane wave spectrum for PMMA gives an Insertion Loss lower than the plane wave result. This in part is due to shift in the apparent position of the source which is of $O(h/R)$ and has been ignored in Eq. (7). The numerical integration also shows a characteristic deviation from the plane wave result at about 55 kHz that agrees well with experiment. This is above the coincidence frequency and the error analysis would need to be extended to investigate this effect.

The error analysis also indicates that the deviations from the plane wave results should be larger for steel and the integrals more difficult to evaluate numerically due to the proximity of the poles to the path of the integral over the evanescent part of the plane wave spectrum when the material damping is small. This is likely to be the cause of the discrepancy between the results of [3] and [4]. The current results show that for realistic separations the deviations from the plane wave results are small. Only at very small source-receiver separations do the deviations become realistically measurable at low frequencies, and then they are unlikely to be of significance.

Acknowledgments

JS was funded by the Defence Technology and Innovation Centre (DTIC).

References

[1] V. F. Humphrey and H. O. Berktay, "The transmission coefficient of a panel measured with a parametric source", *J. Sound Vibr.* **101**, 85-108 (1985).

[2] V. F. Humphrey, "The influence of the plane wave spectrum of a source on measurements of the transmission coefficient of a panel", *J. Sound Vibr.* **108**, 261-272 (1986).

[3] J. C. Piquette, "Spherical-wave scattering by a finite-thickness solid plate of infinite lateral extent, with some implications for panel measurements", *J. Acoust. Soc. Am.* **83**, 1284 (1988).

[4] E. L. Shenderov, "Transmission of a spherical wave through an elastic layer", *Sov. Phys. Acoust.* **37**, 417 (1991).

[5] E. L. Shenderov, "A sound field near an elastic layer excited by a spherical source", *Acoustical Physics* **40**, 414 (1994).

[6] F. W. J. Olver, "Asymptotics and Special Functions", Academic Press. Reprinted by A K Peters, 1997.

[7] D. G. Crighton, "The 1998 Rayleigh medal lecture: fluid loading — the interaction between sound and vibration", *J. Sound Vibr.* **1**, 1-27 (1989).

[8] J. D. Smith, "Symmetric wave corrections to the line driven, fluid loaded, thin elastic plate", *J. Sound Vibr.* **305**, 827-842 (2007).

[9] L. M. Brekhovskikh, "Waves in layered media", London: Academic Press (Second Edition), 1980.

[10] V. F. Humphrey, "The measurement of acoustic properties of limited size panels by use of a parametric source", *J. Sound Vibr.* **98**, 67-81 (1985).